JOURNAL OF SOLID STATE CHEMISTRY 106, 271–281 (1993)

A One-Dimensional Cuprate Closely Related to the "0212"-Structure: $Nd_2Ba_4Cu_2O_9$

B. DOMENGÈS, F. ABBATTISTA,* C. MICHEL, M. VALLINO,* L. BARBEY, N. NGUYEN, AND B. RAVEAU

*Laboratoire CRISMAT, ISMRa, Boulevard du Marechal Juin, 14050 Caen Cedex, France; and *Dipartimento di Scienza dei Materiali e Ingegneria chimica, Politecnico di Torino, Turin, Italy*

Received October 15, 1992; in revised form January 13, 1993; accepted January 15, 1993

The structure of the cuprate $Nd_2Ba_4Cu_2O_9$ has been determined using both X-ray powder diffraction and high resolution electron microscopy. The compound crystallizes in the space group $P\bar{4}n2$ with $a = 12.072$, $c = 3.874$ Å. The structure consists of isolated chains of corner-sharing CuO_5 pyramids whose cohesion is ensured by the presence of Nd^{3+} and Ba^{2+} cations, the coordination of which can be described as distorted monocapped trigonal prisms BaO_7 and NdO_7. A description of the structure in terms of pyramidal copper chains sharing their corners with NdO_5 tetragonal pyramids is also given. The resulting three-dimensional framework $[Nd_2Cu_2O_8]_x$ forms octogonal tunnels where the barium cations and the additional oxygen are located. The close relationships between this one-dimensional cuprate and the layered cuprates are discussed. © 1993 Academic Press, Inc.

Introduction

Investigations performed these last 5 years in the course of research on superconducting cuprates have shown the high potential significance of the systems *A*–*Ln*–Cu–O, in which *A* and *Ln* represent an alkaline earth and a lanthanide element, respectively (for a review see Ref. (*1*)). There is no doubt that the low dimensionality of the structure plays an important role in the appearance of superconductivity. Indeed, all these superconductors exhibit a layer structure, corresponding either to an oxygen-deficient perovskite such as $YBa_2Cu_3O_7$ or to the intergrowth of rock salt layers with oxygen-deficient perovskite layers such as the $La_2SrCu_2O_6$ and $La_{2-x}A_xCuO_4$ families identified long before the discovery of Bednorz and Muller (*2*). Starting from this idea of low dimensionality, many attempts were made to synthesize new phases in these systems. Two layered cuprates were then isolated: $Ln_{1-x}Ce_x(Ba_{1-y}Ln_y)_2Cu_3O_{10}$ (*3*, *4*) corresponding to the intergrowth of the "123" layers with double fluorite layers, and the oxide $Nd_{2.64}Sr_{0.82}Ce_{0.54}Cu_2O_{8-y}$ (*5*, *6*), corresponding to the triple intergrowth of oxygen deficient perovskite, rock salt, and fluorite layers. Although they do not superconduct when synthesized under normal oxygen pressure, these oxides can be considered as potential superconductors, since superconductivity can be induced by applying oxygen pressure of several hundred bars, as has been shown for $Ln_{1-x}Ce_x(Ba_{1-y}Ln_y)_2Cu_3O_{10}$, for which critical temperatures of 36 to 43 K can be reached (*3*, *4*).

Up to now, no effort has been made to decrease further the dimensionality of the structure in these cuprates, i.e., to generate structures characterized by isolated copper chains. In this respect, the alkaline earth neodymium cuprates are interesting materials, as shown for the oxides $Sr_6Nd_3Cu_6O_{17}$ (*7*, *8*) and $Sr_{2-x}Nd_{1+x}Cu_2O_{6-y}$ (*8*, *10*). Indeed, the structures of both cuprates exhibit a lower dimensionality than that of layer

0022-4596/93 $5.00

cuprates: $Sr_6Nd_3Cu_6O_{17}$ consists of "123" ribbons isolated from each other by rock salt layers, whereas $Sr_2NdCu_2O_{6-y}$ forms six-sided tubes of copper polyhedra isolated from each other by rock salt layers and neodymium layers. Thus these two structures can be considered as intermediate between a pure layer and a pure chain structure. For these reasons it was decided to investigate the system Ba–Nd–Cu–O (*11*). We report here on the crystal structure of the cuprate $Nd_2Ba_4Cu_2O_9$ which is to our knowledge the first cuprate with a chain-like structure isolated up to now.

Experimental

The cuprate $Nd_2Ba_4Cu_2O_9$ was synthesized according to the protocol previously described (*11*). Its synthesis requires the utmost precautions to avoid contamination with CO_3^{2-} ions, both from starting materials ($Ba(NO_3)_2$, CuO, Nd_2O_3) and from the sintering atmosphere (flowing high-purity oxygen, $CO_2 < 1$ ppm). This $Nd_2Ba_4Cu_2O_9$ sample was finally heated to 950°C in oxygen, then slowly furnace cooled to room temperature.

The XRD pattern was registered by means of a Seifert vertical goniometer equipped with a primary monochromator in order to select the $CuK_{\alpha 1}$ radiation. Data were collected in the range $20° \leq 2\theta \leq 100°$ by step scanning, with increment 0.02° (2θ). Lattice constants were refined and structural calculations were performed using the profile analysis computer program DBW 3.2 (*12*).

For electron microscopy study, the sample was gently ground in *n*-butanol and deposited on a holey carbon-coated nickel grid. Electron diffraction work was performed on a side entry JEM 200 CX equipped with a tilting rotating sample holder, which allowed the reciprocal space to be reconstructed. High resolution work was performed with an Akashi 2B equipped with a double tilt sample holder (±10°) and with objective lens spherical aberration constant $C_s = 0.4$ mm. Energy-dispersive X-ray spectroscopy analyses were also performed on this microscope, most often using a 6 nm diameter nanoprobe. HREM images were calculated using the multislice method of the EMS program (*13*).

The magnetic susceptibility was measured in the temperature range 4–500 K with a Faraday balance under a magnetic field $H = 3$ kG.

Structural Study

The preliminary transmission electron microscopy investigation and the EDS analyses confirm the tetragonal symmetry of this phase, i.e., $a \approx 12$, $c \approx 3.9$ Å, and its cationic composition, leading to the previously established formula $Nd_2Ba_4Cu_2O_9$ (*11*). In addition, they evidence the reflection conditions $0kl$ $k + l = 2n$ (Fig. 1), leading to three possible space groups, $P4_2nm$, $P\bar{4}n2$, and $P4_2/mnm$; moreover a second phase,

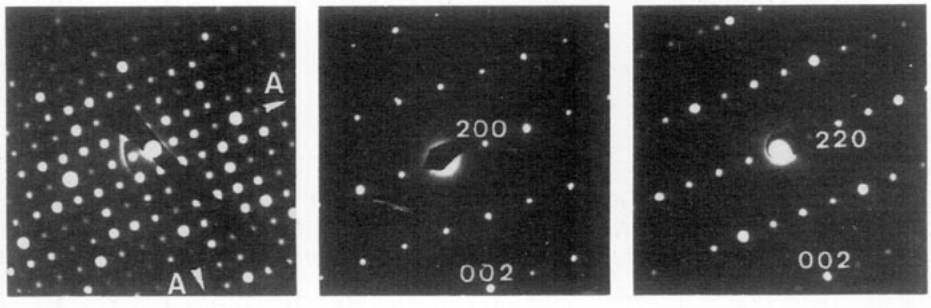

FIG. 1. Characteristic E.D. patterns of $P\bar{4}n2$ space group, showing the following reflection conditions: $hk0$, no; $h0l$, $h + l = 2n$; hhl, no.

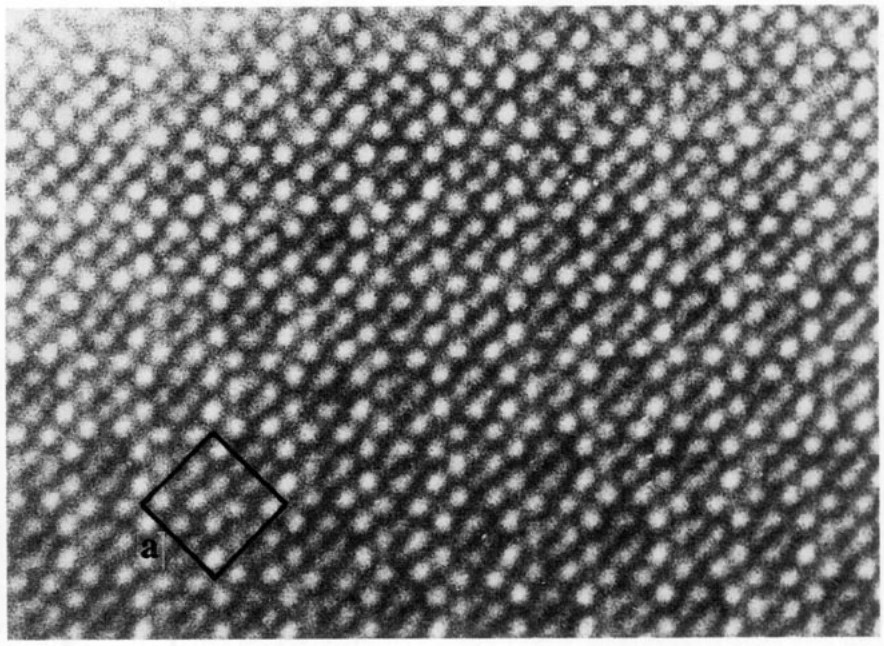

FIG. 2. Characteristic high resolution electron microscopy (001) image of $NdBa_2CuO_{4.5}$ sample.

Nd_2BaCuO_5, was detected as a minor impurity. A typical high resolution electron microscopy image of experimental through focus series shows a centered array of groups of four bright dots (Fig. 2). Parallely to the ⟨110⟩ direction each group is alternately clockwise and counter clockwise rotated around the **c** axis. Between these bright dots, groups of grey spots forming diamonds are observed. Considering the experimental through focus series, the high electron density zones were supposed to be highlighted on this image and the groups of four bright dots were related to barium atoms. On the other hand, picnometric measurements established the formula $Ba_8Nd_4Cu_4O_{18.3}$ per cell (*11*), i.e., 8 barium atoms per cell. Thus, geometry and symmetry considerations made the $P\bar{4}n2$ space group appear most probable; it was chosen for structure calculations, Nd_2BaCuO_5 being introduced as a secondary phase.

The cell parameters were refined from X-ray powder diffraction patterns to a = 12.0717 (2) and c = 3.8737 (1) Å. Note the value of the c parameter close to the a parameter of the perovskite which allowed CuO_6 octahedra or CuO_5 pyramids to be suggested for the structure. No isostructural phase being known, Fourier maps were used in addition to profile analysis to determine the structure of the $Nd_2Ba_4Cu_2O_9$ compound. Based on HREM images, the barium atoms were assumed to be located in the **8i** sites of the $P\bar{4}n2$ space group, with $x \approx 0.1$, $y \approx 0.2$, $z = 0.75$, which lead to the different R factors given in Table I. Then Fourier difference sections revealed peaks close to $x = 0.40$, $y = 0.10$, $z = 0.25$ and $x = 0.10$, $y = 0.40$, $z = 0.25$, which were attributed to neodymium and copper, respectively,

TABLE I

AGREEMENT FACTOR VALUES AFTER SUCCESSIVE INTRODUCTION OF METALLIC ATOMS INTO THE CALCULATION

Atoms	Site	x	y	z	R_p (%)	R_{wp} (%)	R_i (%)
Ba	8i	0.1	0.2	3/4	19.04	31.63	82.57
+Nd	4f	0.4	0.1	1/4	13.92	19.67	49.36
+Cu	4f	0.1	0.4	1/4	10.59	14.06	24.21

owing to their relative intensity. A calculated XRD pattern performed with Nd and Cu located in the **4f** sites led to significant decreases of the different R factors (Table I). New Fourier sections, including all the metallic atoms, were then calculated to determine the oxygen positions. From the observed peaks, four sets of oxygen sites could be observed:

$$\text{O1...}\mathbf{4g}\left(x, \frac{1}{2}+x, \frac{1}{4}\right) \text{ with } x \sim 0.4$$

$$\text{O2...}\mathbf{2b}\left(0, 0, \frac{1}{2}\right)$$

$$\text{O3...}\mathbf{4f}\left(x, \frac{1}{2}-x, \frac{1}{4}\right) \text{ with } x \sim \frac{1}{4}$$

$$\text{O4...}\mathbf{8i}\,(x, y, z) \text{ with } x \sim 0,\ y \sim \frac{1}{4},\ z \sim \frac{1}{4}$$

Calculations were then performed with all the atoms. After successive refinements of the positional parameters and of the isotropic thermal factors, the different agreement factors were minimized to R_p = 5.72%, R_{wp} = 7.28%, R_i = 8.19% for the values of the set of variable parameters given in Table II. Figure 3 shows the experimental, calculated, and difference XRD patterns, which attest the validity of the fit.

TABLE II

REFINED VALUES OF THE DIFFERENT VARIABLES FOR $Nd_2Ba_4CuO_9$: SPACE GROUP $P\bar{4}n2$

Atom	Site	x	y	z	B (Å^2)
Ba	8i	0.1132 (3)	0.1761 (3)	0.75	0.9 (1)
Nd	4f	0.3879 (3)	0.1121 (3)	0.25	0.8 (1)
Cu	4f	0.1005 (6)	0.3995 (6)	0.25	0.6 (2)
O(1)	4g	0.404 (2)	0.904 (2)	0.25	0.8 (7)
O(2)	2d	0	0	0.5	0.1 (8)
O(3)	4f	0.245 (2)	0.255 (2)	0.25	0.1 (7)
O(4)	8i	−0.026 (2)	0.300 (2)	0.25	0.3 (5)

R_p = 5.72%, R_{wp} = 7.28%, R_i = 8.19%

Attempts to displace barium or O(4) atoms along **c** from their position do not result in a significant variation of the R factors.

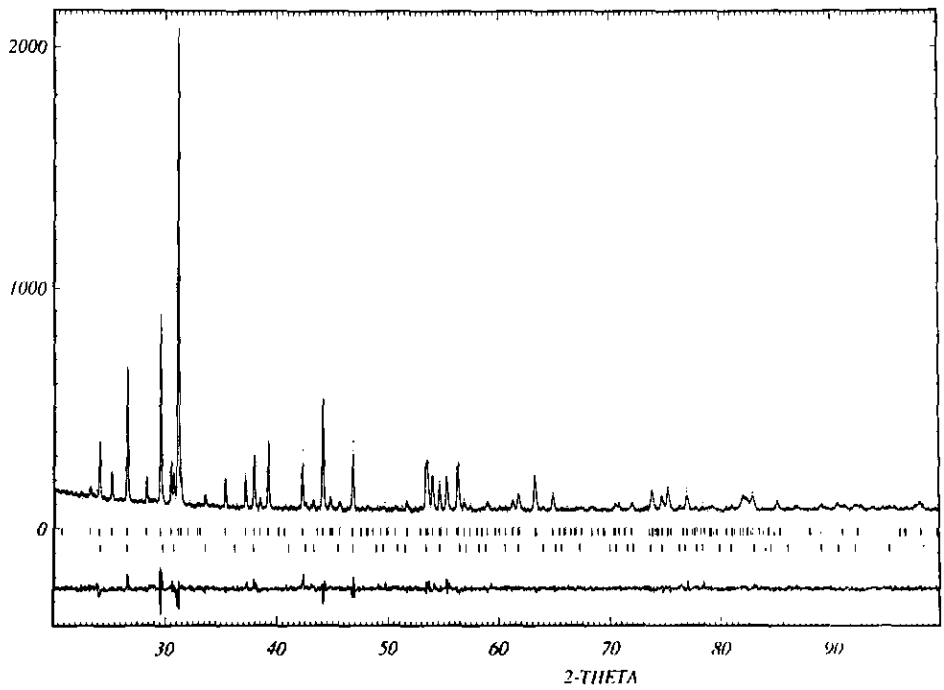

FIG. 3. X-ray powder diffraction $NdBa_2CuO_{4.5}$ patterns: experimental, calculated, and difference.

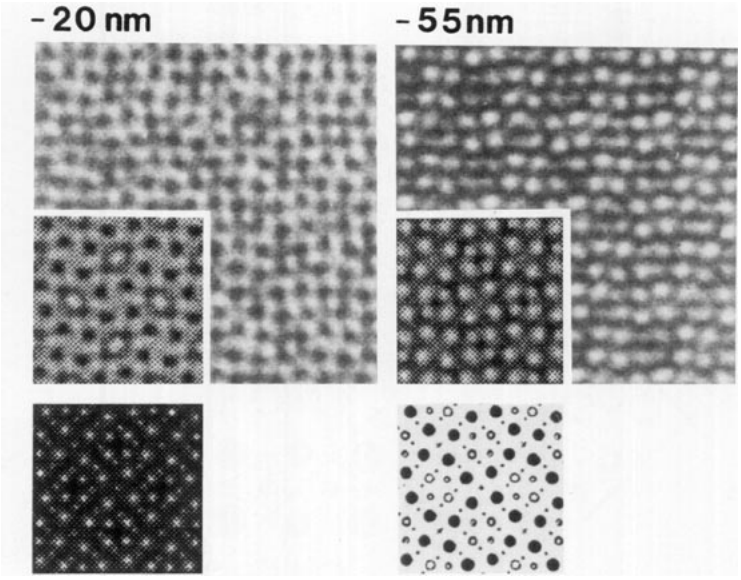

FIG. 4. Characteristic HREM (001) images of experimental through-focus series. Calculated images are enclosed in experimental ones. Calculation parameters are high voltage $V = 200$ kV, spherical aberration constant $C_s = 0.4$ mm, half-angle convergence $\alpha = 0.85$ mrad, spread of focus $\Delta = 10$ nm, crystal thickness $T = 3.1$ nm, focus -20 and -55 nm. Projected potential and (001) projection of the structure are also given.

In order to support the X-ray powder diffraction results, high resolution electron microscopy (001) image calculations have been performed based on the structural parameters of Table II (Fig. 4). Considering the (001) projected potential of the $Nd_2Ba_4Cu_2O_9$ structure, four different infinite rows parallel to **c** can be distinguished: Ba atom rows, Nd atom rows, Cu–O infinite rows, and infinite O atom rows. The calculated images are in good agreement with the experimental ones. Typical images of the through-focus series are given (Fig. 4). For -20 nm focus value low electron density zones are highlighted and bright dots built up a light map contrast corresponding to oxygen atoms and oxygen vacancy. Ba atoms thus appear as very dark dots, Cu–O infinite rows as smaller dark dots, and Nd atoms as grey dots. For -55 nm focus value, high electron density zones are highlighted and the group of four bright dots can be ascribed to Ba atom rows and greyer dots forming diamonds to Nd and CuO rows, in agreement with preliminary interpretation. Most of the crystals showed very neat defect-free contrast.

Description of the Structure and Discussion

The projection of the structure of this phase along **c** (Fig. 5) shows that it consists of $[CuO_4]_\infty$ chains of corner-sharing CuO_5 pyramids running along **c**, whose cohesion is ensured by neodymium and barium cations. Two chains of pyramidal copper face each other through the basal plane of their CuO_5 pyramids (Fig. 6) exactly as in the layered cuprates involving double pyramidal copper layers. Thus in each pair of pyramidal copper chains the copper atoms are sitting at the same level along **c**. In the structure these pairs of pyramidal Cu chains are located at two levels in such a way that each pair of Cu chain is surrounded by four pairs **c**/2 translated and 90° rotated (Fig. 5).

The CuO_5 pyramids exhibit four basal Cu–O distances close to 1.94 Å (Table III) and one Cu–O apical bond, oriented along

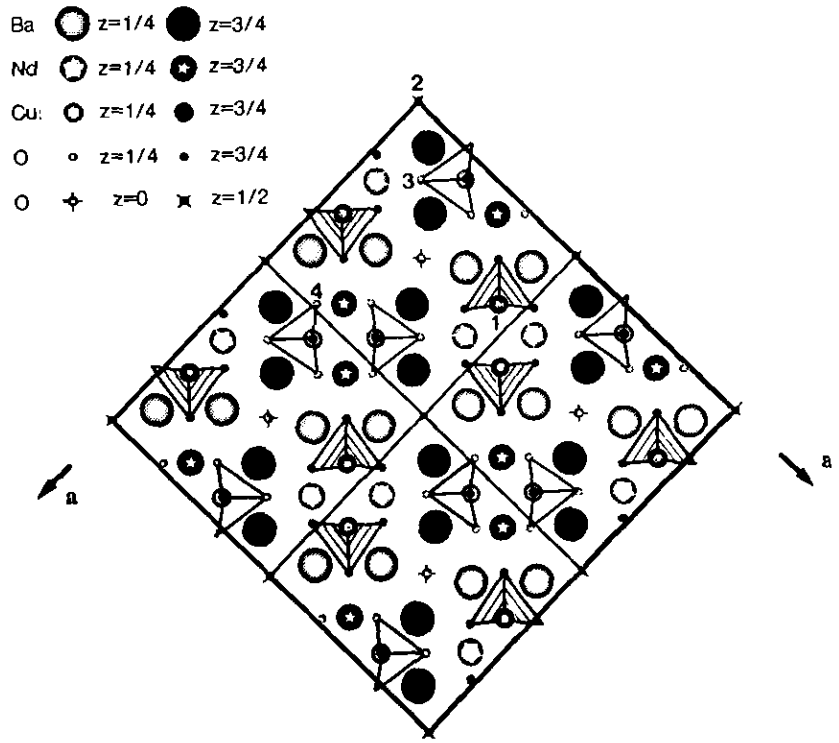

FIG. 5. (001) projection of $NdBa_2CuO_{4.5}$ structure (four cells). CuO_5 pyramids are drawn, and those corresponding to $z_{Cu} = 3/4$ are hatched. The four oxygen sites are indicated by their number. Atom symbols will be kept on following drawings.

⟨110⟩, of 2.46 Å, in agreement with the distances usually observed in other cuprates.

The neodymium atoms are located between the pyramidal chains in the same position with respect to the CuO_5 pyramids (Fig. 6) as in the cuprates with double pyramidal copper layers. The pairs of pyramidal Cu chains being isolated in $Nd_2Ba_4Cu_2O_9$, the Nd atoms exhibit only seven oxygen neighbors instead of eight as in layered cuprates (Fig. 7). Thus Nd keeps six of its usual oxygen neighbors; as a matter of fact, only half of the square prismatic coordination polyhedron is remaining, i.e., a trigonal prism built

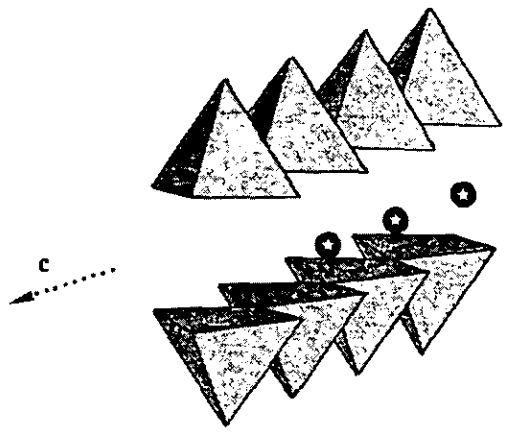

FIG. 6. Perspective view of a pair of infinite pyramidal copper chains parallel to c.

TABLE III

INTERATOMIC DISTANCES (IN Å)

Ba–O(1)	2.76 (3) × 1	Cu–O(1)	1.94 (1) × 2
O(2)	2.71 (1) × 1	O(3)	2.46 (2) × 1
O(3)	2.68 (2) × 2	O(4)	1.94 (2) × 2
O(4)	2.90 (2) × 1		
O(4)	2.97 (2) × 2		
Nd–O(1)	2.52 (3) × 2	Cu–Cu	3.43 (1)
O(3)	2.45 (2) × 1	O(1)–O(1)	3.27 (4)
O(4)	2.44 (1) × 4	O(4)–O(4)	2.96 (3)

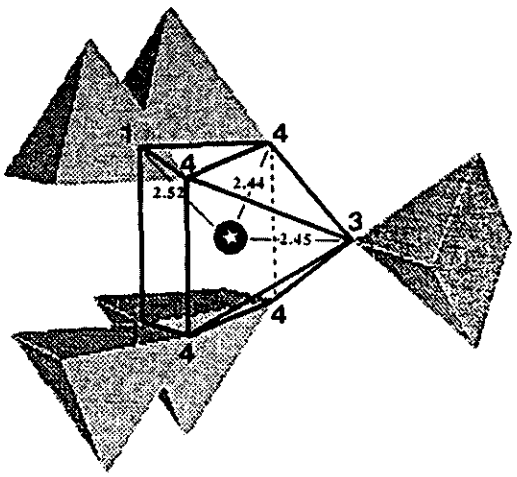

FIG. 7. Nd environment. The seven oxygen neighbors, corresponding to the drawn polyhedron corners, are identified by their numbers. The CuO_5 pyramids which they belong to are shaded.

up from O(4) and O(1) oxygen atoms (Fig. 7). More precisely, Nd is located at the center of a rectangle characterized by four Nd–O(4) distances of 2.44 Å; it exhibits two slightly longer Nd–O(1) bonds of 2.52 Å with the O(2) oxygen atoms of the facing CuO_5 pyramids, sitting at the same level z. The seventh near neighbor, namely the O(3) apical oxygen atom of the CuO_5 pyramid, makes it possible to achieve a distorted monocapped trigonal prismatic coordination, which is similar to that observed in the $Sr_2NdCu_2O_6$ structure (*8*). Another description of the coordination polyhedron of Nd consists in considering the existence of NdO_5 tetragonal pyramids (Fig. 7). In both cases—trigonal prism and tetragonal pyramid—Nd sits at the center of the rectangular O(4) face. From this, the overall sevenfold coordination of Nd is better understood in terms of a complex polyhedron resulting from the rectangular face sharing of a tetragonal pyramid and a trigonal prism (Fig. 7). Taking into consideration the shortest Nd–O distances, i.e., smaller than 2.5 Å, it is worth pointing out that the structure can be described as a three-dimensional array of CuO_5 and NdO_5 pyramids sharing their corners in the (001) plane (Fig. 8) in such a way that one CuO_5 pyramid alternates with

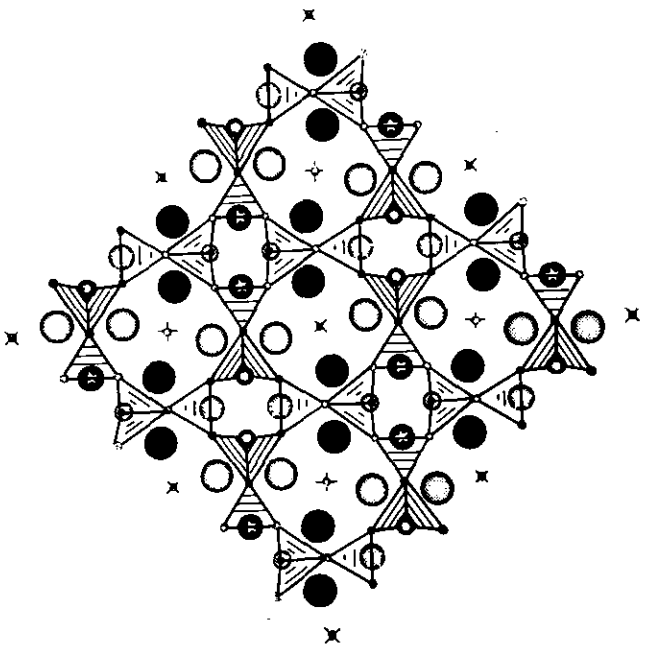

FIG. 8. (001) projection of $NdBa_2CuO_{4.5}$ structure showing the three-dimensional framework of CuO_5 and NdO_5 pyramids. Pyramid faces are more or less strongly hatched depending to their mean z level.

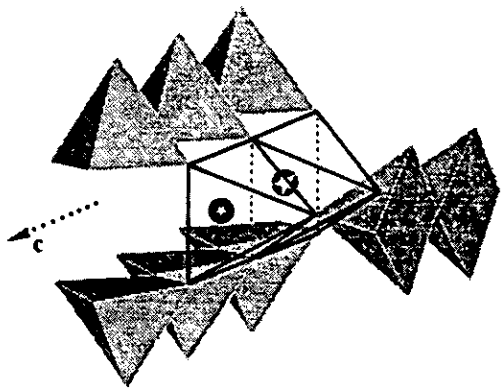

FIG. 9. Perspective view showing the stacking of NdO_5 and CuO_5 pyramids along c: face-sharing and corner-sharing respectively.

one NdO_5 pyramid; i.e., each CuO_5 pyramid is linked to five NdO_5 pyramids and reciprocally. Along **c** the CuO_5 pyramids share their corners, whereas the NdO_5 pyramids share their edges (Fig. 9). This explains the stability of this structure, whose three dimensional framework $[Cu_2Nd_2O_8]_\infty$ forms octogonal tunnels running along **c** where barium and oxygen atoms are located (Fig. 8).

The barium atoms, like the neodymium ones, have seven oxygen neighbors (Fig. 10). The Ba–O bond lengths rather correspond to a 4 + 3 coordination with four short distances close to 2.7 Å—oxygen atoms O(1) · O(3) · O(3) · O(2) forming a distorted trigonal pyramid—and three longer distances BaO(4) close to 3 Å. The barium sevenfold coordination can be also described as a strongly distorted monocapped trigonal prism BaO_7. A partial perspective view of the structure (Fig. 10) shows that each trigonal BaO_6 prism has one rectangular face (built up from two O(3) and two O(4) atoms) and its two triangular face (built up from two O(4) and one O(2) atoms or from two O(3) and one O(4) atoms, respectively) perpendicular to the (001) plane, whereas the additional oxygen O(1) forming the BaO_7 group belongs to the basal plane of the CuO_5 pyramid. The arrangement of the BaO_6 prisms (Fig. 11) shows they form a three-dimensional framework which also supports the stability of the structure. One can indeed observe that the BaO_6 distorted prisms form rows running along the ⟨110⟩ directions. These rows have their bariums atom located at two different levels shifted by **c**/2: the Ba rows located at $z = 1/4$ run along $[1\bar{1}0]$, whereas those located at $z = 3/4$ run along [110]. Thus, two rows of different levels ($z = 1/4$ and $z = 3/4$) are 90°-rotated and intersect at the center of the octogonal tunnel described above, so that the O(2) atom located at the center of these tunnels is shared between four BaO_6 prisms (two with $z_{Ba} = 1/4$ and two with $z_{Ba} = 3/4$) (Fig. 11b). In each row, the BaO_6 prisms alternately share one corner and one edge along **c**, whereas a BaO_6 prisms of one row shares two edges (O(2)–O(4)) with two BaO_6 prisms of the adjacent 90° rotated row.

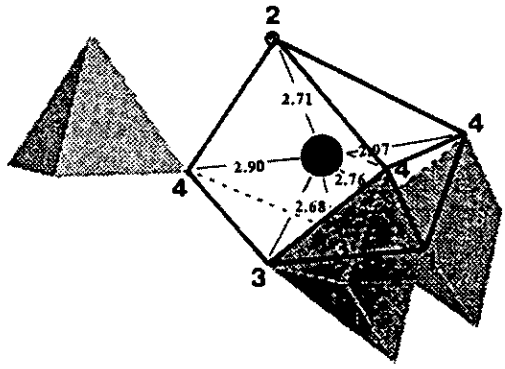

FIG. 10. Ba environment. The seven oxygen neighbors, corresponding to the drawn polyhedron corners, are identified by their numbers and the CuO_5 pyramids which they belong to are shaded.

In fact this structure is closely related to those of the layered cuprates involving double pyramidal copper layers, as for instance $La_2CaCu_2O_6$. In both structures (Fig. 12) one recognizes similar infinite unidimensional units built up from double pyramidal copper chains and involving two rows of Nd atoms (or Ca) and four rows of barium (or lanthanum) atoms running along these chains, i.e. along **c** for $Ba_4Nd_2Cu_2O_9$ or along **a** for $La_2CaCu_2O_6$. In $La_2CaCu_2O_6$ such infinite unidimensional units share their edges, forming layers (Fig. 12a), two succes-

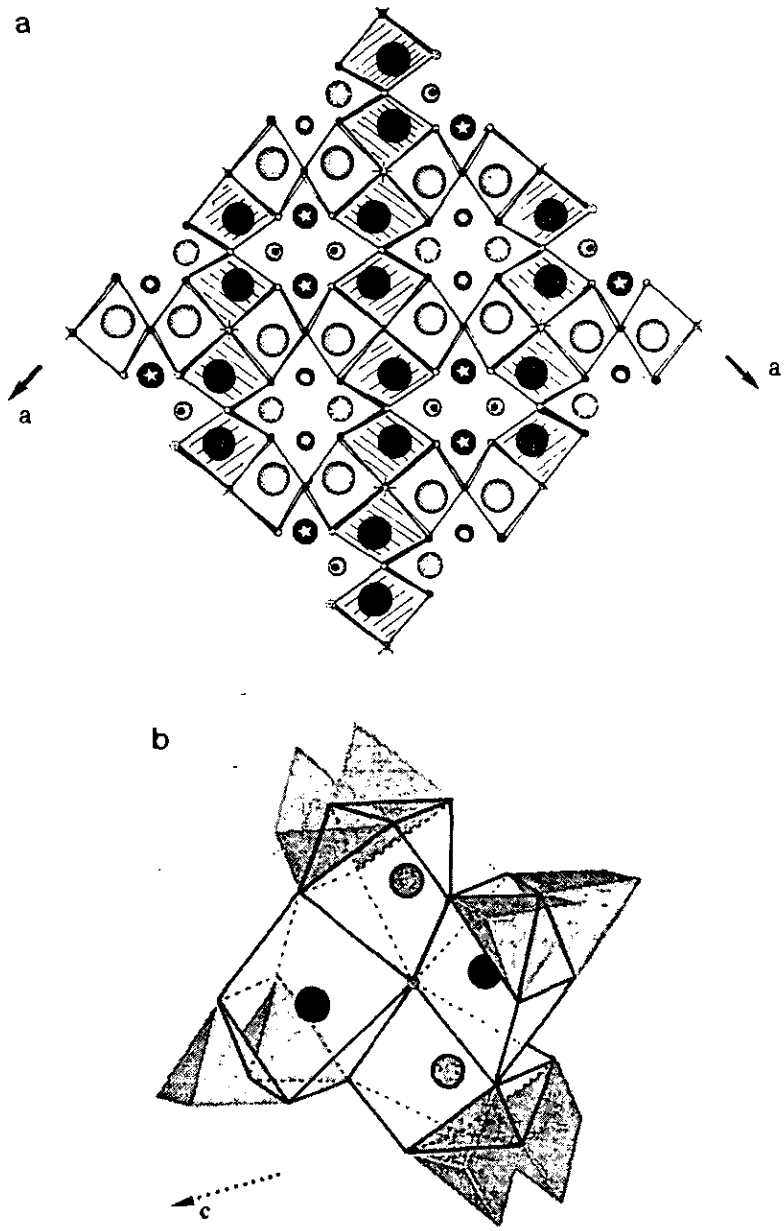

FIG. 11. (a) (001) projection of $NdBa_2CuO_{4.5}$ structure showing rows of BaO_6 distorted prisms parallel to ⟨110⟩. Pseudorectangular faces of prisms corresponding to $z_{Ba} = 3/4$ are hatched. The prism trigonal faces parallel to **c** are thickened and for the prism corresponding to $z_{Ba} = 3/4$ they are darkened. (b) Perspective view showing the connection between four adjacent BaO_7 polyhedra sharing the O(2) atom. Neighboring CuO_5 pyramids are shaded.

sive layers being shifted by **a**/2. In $Ba_4Nd_2Cu_2O_9$ the different infinite unidimensional units are all disconnected; each unit is surrounded by four similar units turned 90° and shifted by **c**/2 (Fig. 12b). This relationship suggests the possible existence of new phases as intergrowths between the two structures.

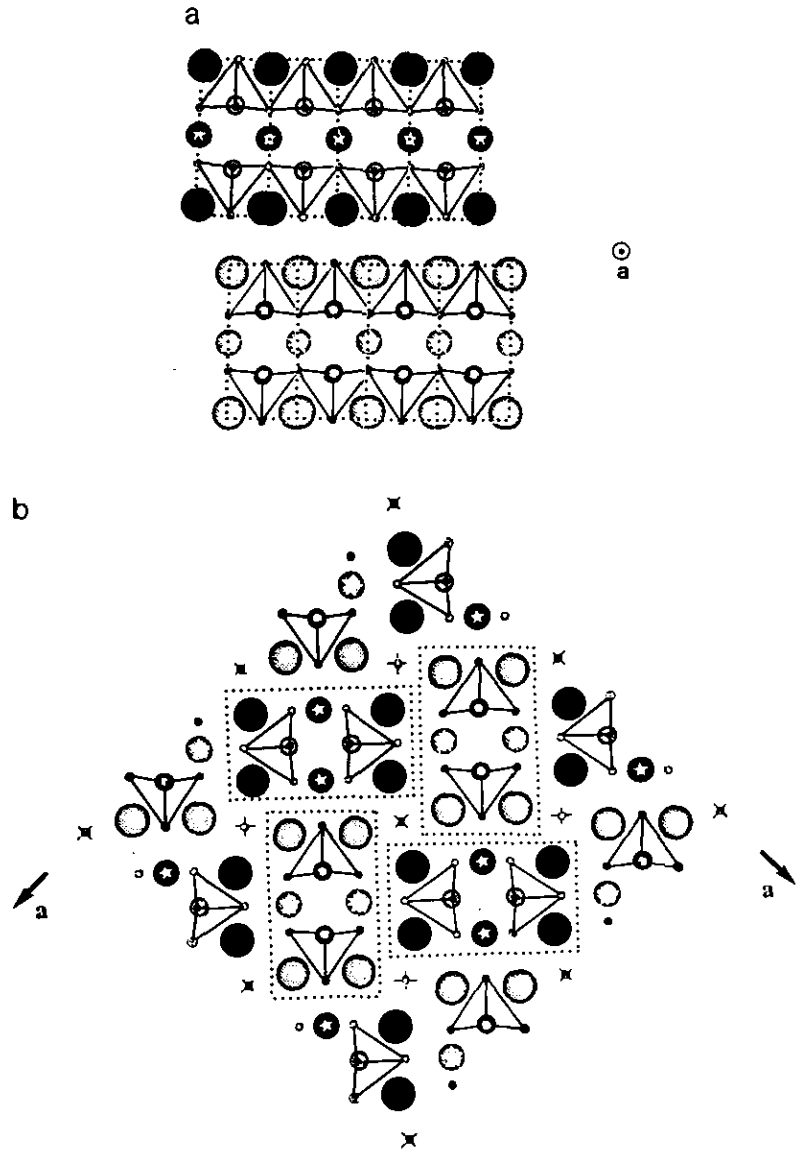

FIG. 12. (a) (100) projection of the $La_2CaCu_2O_6$ structure showing the stacking of infinite unidimensional $A_4A'Cu_2O_8$ units of double pyramidal copper chains. (b) (001) projection of the $Ba_4Nd_2Cu_2O_9$ structure showing the stacking of infinite unidimensional $Ba_4Nd_2Cu_2O_8$ units of double copper pyramidal chains.

Although this material can be considered as a potential superconductor, electrical measurements show that it is a poor semiconductor, in agreement with the fact that copper is in the divalent state. The magnetic measurements confirm this property. The inverse susceptibility vs temperature curve obeys the Curie–Weiss law from 70 K, with a negative paramagnetic Curie temperature. One observes good agreement between experimental and theoretical molar values of the Curie constant ($4.0\,\mu_B^2$ and $4.25\,\mu_B^2$ respectively) taking $\mu_{eff}(Nd^{3+}) = 3.66\,\mu_B$ and $\mu_{eff}(Cu^{2+}) = 1.9\,\mu_B$.

Concluding Remarks

A cuprate with a chain-like structure has been observed for the first time. Although the preliminary measurements evidence semiconducting behavior, in agreement with the presence only of Cu(II), the possibility of superconductivity in this structure cannot so far be excluded. Attempts at doping and also at synthesis under high oxygen pressure will be performed in order to induce superconductivity. Moreover, owing to its close relationships with layered cuprate, this new structural type opens the route to the research of new compounds with a network intermediate between the pure chain-like and layered structures.

References

1. B. Raveau, C. Michel, M. Hervieu, and D. Groult, *"Crystal Chemistry of High-T_c Superconducting Copper Oxides,"* Springer Series in Materials Science (H. K. V. Losch, Ed.), Vol. 15, Springer-Verlag, Berlin/New York (1991).
2. J. G. Bednorz and K. A. Muller, *Z. Phys. B* **64,** 189 (1986).
3. H. Sawa, K. Obara, J. Akimitsu, Y. Matsui, and S. Horiuchi, *J. Phys. Soc. Jpn.* **58,** 2252 (1989).
4. T. Wada, A. Ichinose, Y. Yaegashi, Y. Yamauchi, and S. Tanaka, *Phys. Rev. B* **41,** 1984 (1990).
5. J. Akimitsu, S. Suzuki, M. Watanabe, and H. Sawa, *Jpn. J. Appl. Phys.* **27,** L1859 (1988).
6. H. Sawa, S. Suzuki, M. Watanabe, J. Akimitsu, H. Matsubara, H. Watabe, S. Uchida, K. Kusho, H. Asano, F. Izumi, and E. Takayama-muromachi, *Nature* **337,** 347 (1989).
7. V. Caignaert, R. Retoux, M. Hervieu, C. Michel, and B. Raveau, *J. Solid State Chem.* **91,** 41 (1991).
8. V. Caignaert, R. Retoux, M. Hervieu, C. Michel, and B. Raveau, *Physica C* **167,** 483 (1990).
9. J. R. Grasmeder and M. T. Weller, *J. Solid State Chem.* **85,** 88 (1990).
10. R. A. Steadman, D. M. de Leeuw, G. P. Geelen, and E. Fikkee, *Physica C* **162–164,** 542 (1989).
11. F. Abbattista, D. Mazza, and M. Vallino, *Eur. J. Solid State Inorg. Chem.* **28,** 649 (1991).
12. D. B. Wiles and R. A. Young, *J. Appl. Crystallogr.* **14,** 149 (1981).
13. P. A. Stadelmann, *Ultramicroscopy* **21,** 131 (1987).